

Regulatory Efficacy of Brown Seaweed *Lessonia nigrescens* Extract on the Gene Expression Profile and Intestinal Microflora in Type 2 Diabetic Mice

Chao Zhao, Chengfeng Yang, Mingjun Chen, Xucong Lv, Bin Liu, Lunzhao Yi, Laura Cornara, Ming-Chi Wei, Yu-Chiao Yang, Rosa Tundis, and Jianbo Xiao*

Scope: In this study, the antidiabetic activity of *Lessonia nigrescens* ethanolic extract (LNE) is investigated in streptozotocin (SZT)-induced type 2 diabetic mice fed with a high-sucrose/high-fat diet.

Methods and results: Ultra high performance liquid chromatography coupled with photo-DAD and electrospray ionization–mass spectrometry (ESI–MS) is employed to analyze the major compounds in LNE. The components of the intestinal microflora in type 2 diabetic mice are analyzed by high-throughput next-generation 16S rRNA gene sequencing. Fasting blood glucose levels in diabetic mice are significantly decreased after LNE administration. The histology reveals that LNE could protect the cellular architecture of liver and kidney. LNE treatment significantly increases *Bacteroidetes* and decreases *Firmicutes* populations in intestinal microflora. Specifically, It could selectively enrich the amounts of beneficial bacteria, *Barnesiella*, as well as reduce the abundances of *Clostridium* and *Alistipes*. The increased gene and protein expression levels of phosphatidylinositol 3-kinase (PI3K) in the liver are observed in LNE treatment groups, while the expressions of c-Jun N-terminal kinase (JNK) are significantly downregulated.

Conclusion: The above findings suggest that LNE could be considered as a functional food for reducing blood glucose and regulating intestinal microflora.

1. Introduction

Diabetes mellitus, one of the most important global public health problems, has been the leading cause of death worldwide. According to the International Diabetes Federation it has been estimated that, in 2015, the number of adults with diabetes was 415 million, which will increase to 642 million by 2040,^[1] with China, India, and USA as the top three countries contributing to half of the global population of diabetes.^[2] Diabetes is mainly characterized by hyperglycemia, in particular, type 2 diabetes is the most common form of diabetes accounting for approximately 90% of all cases.^[3] Accumulating evidence indicates that the intestinal microflora composition is associated with the development of type 2 diabetes,^[4] which has been considered to be a new therapeutic target for prevention and management of the disease.^[5] Hence, effective control of blood glucose levels and regulation

Dr. C. Zhao, Dr. C. Yang, M. Chen, Dr. X. Lv, Prof. B. Liu
College of Food Science
Fujian Agriculture and Forestry University
Fuzhou, China

Dr. C. Zhao
Department of Chemistry
University of California
Davis, CA, USA

Dr. C. Zhao
Fujian Province Key Laboratory for the Development of Bioactive Material
from Marine Algae
Quanzhou Normal University
Quanzhou, China

Prof. L. Yi
Yunnan Food Safety Research Institute
Kunming University of Science and Technology
Kunming, China

Prof. L. Cornara
Dipartimento di Scienze della Terra dell'Ambiente e della Vita
Università degli Studi di Genova
Genova, Italy

Prof. M.-C. Wei
Department of Applied Geoinformatics
Chia Nan University of Pharmacy and Science
Tainan, Taiwan

Prof. Y.-C. Yang
Department and Graduate Institute of Pharmacology
Kaohsiung Medical University
Kaohsiung, Taiwan

Prof. R. Tundis
Department of Pharmacy
Health and Nutritional Sciences
University of Calabria
Arcavacata Rende, Italy

Dr. J. Xiao
Institute of Chinese Medical Sciences
State Key Laboratory of Quality Control in Chinese Medicine
University of Macau, Avenida da Universidade
Macau, China
E-mail: jianboxiao@yahoo.com

DOI: 10.1002/mnfr.201700730

of intestinal microbial community are important aspects of preventing or reversing the onset of type 2 diabetes.

The microbial inhabitants of the gut have an influence on the onset of diabetes. Gut microbial dysbiosis has also appeared in diabetes. The gut microbiome of patients with type 2 diabetes harbored lower levels of select short-chain fatty acid-producing bacteria and higher levels of potential opportunistic pathogens.^[6] Changes in gut microbiota contribute to increases in plasma glucose concentrations.^[7] Furthermore, The phosphatidylinositol 3-kinase (PI3K) signaling pathway is considered to play a vital role in insulin signal transduction that is essential for body glucose homeostasis through glucose uptake in periphery.^[8] Upon insulin stimulation, the insulin receptor phosphorylates insulin receptor substrate at tyrosine sites, which consequently activates PI3K. Then, PI3K converts phosphatidylinositol-4,5-bisphosphate into phosphatidylinositol-3,4,5-trisphosphate, which may act as the second messenger to activate AKT (protein kinase B). Subsequently, the activated AKT further activates mTOR, which is involved in fundamental cellular processes. Moreover, the molecules c-Jun N-terminal kinases (JNKs) are named after their capacity to phosphorylate and activate the protein cJun, a member of the activator protein-1 family of transcription factors. The JNK pathways are more closely related to glycometabolism than lipid metabolism. Also the abnormally elevated JNK activity is recognized to involve in insulin resistance and β -cell function, which contribute to type 2 diabetes.^[9,10]

Brown algae have a variety of biologically active compounds such as pigments, fucoidans, phycocolloids, and phenolic compounds with diverse bioactivity.^[11] *Lessonia nigrescens* inhabits rocky intertidal and shallow subtidal zone, being a crucial brown algae to ecology and economy.^[12] It contains a broad range of bioactive compounds, such as fucans and phlorotannins.^[13] In this study, the type 2 diabetes mellitus model was established by feeding mice with a high-sucrose/high-fat diet (HSFD) in combination with injection of streptozocin, then the effect of *L. nigrescens* ethanolic extract (LNE) on related signaling pathway and intestinal microflora in diabetic mice was explored. It is the first report of regulatory efficacy of LNE on the gene expression profile and intestinal microflora in vivo. The purpose of this study is to investigate the molecular mechanism underlying the hypoglycemic potential of LNE in type 2 diabetic mice.

2. Experimental Section

2.1. Preparation of Ethanolic Extract from *L. nigrescens*

The clean and air-dried powder (10 g) of *L. nigrescens*, purchased from Qingdao Lanbao Marine Bio-technology Co., Ltd (Qingdao, China), was extracted with 55% ethanol (200 mL) by ultrasound-assisted extraction (50 °C, 45 kHz) for 60 min. The extract was then concentrated and freeze dried. The dried powder was weighed and dissolved in ethanol to obtain the desired experimental concentration and sterilized by passing through a 0.2- μ m filter.

2.2. LC–MS Analysis

The Waters Acquity™ ultra-performance liquid chromatography (UPLC) with photo-DAD was used. The ACQUITY UPLC HSS T3 column (1.8 μ m, 2.1 \times 100 mm) was utilized at 45 °C. The mobile phases were solvent A (water with 0.1% (v/v) formic acid) and solvent B (acetonitrile with 0.1% (v/v) formic acid). The gradient duration was 20 min at a flow rate of 0.45 mL min⁻¹. From the initial to 0.25 min, the column was eluted with 99% solvent A, then was linearly decreased to 1% in 16 min. After that, the eluent was kept at 95% in 0.75 min and finally raised to 99% at the end of a gradient of 5 min period. The injection volume was 1 μ L aliquot of each sample. The photo-DAD was set to a wavelength of 200–600 nm. The UPLC system equipped with a Waters UPLC SYNAPT G2-Si HDMS ESI ion source operating in positive ion mode was used. The m/z range was acquired from 50–1200 Da using the lockspray mode with Leu-enkephalin as the external reference compound. The conditions used for the ESI source were as follows: ion source temperature of 120 °C, desolvation temperature of 800 °C, desolvation gas flow rate of 800 L h⁻¹, cone gas flow of 50 L h⁻¹, sample cone voltage of 45 V, source offset of 80 V, nebulizer gas flow of 6.5 Bar, capillary voltage of 3.0 kV, collision energy ramp of 10–40 eV, and scan time of 0.2 s.

2.3. Animals Experiments

ICR male mice (Specific Pathogen Free, 8-week-old; 18–22 g) were purchased from Fuzhou General Hospital of Nanjing Military (Fuzhou, China). Animals were fed with standard chow diet and water ad libitum and housed in sanitized polypropylene cages in a well maintained and hygienic environment (temperature 27 \pm 1 °C; 60 \pm 10% humidity; and a 12 h/12 h light/dark cycle). All experimental procedures followed the rules of the Guide for the Care and Use of Laboratory Animals published by the US National Institutes of Health (NIH Publication No. 85–23, revised 1996), and were performed in strict accordance with the China legislation regarding the use and care of laboratory animals. The ethical review board of Fuzhou General Hospital of Nanjing Military Command provided ethical approval (number FZJQ2011018). After one week, ten mice were randomly chosen as normal group fed with standard chow, the other 40 mice in the experimental group were fed a HSFD (15% lard, 15% sucrose, 1% cholesterol, 10% yolk, 0.2% sodium deoxycholate, and 58.8% standard chow) to induce diabetes. After 5 weeks, all mice were fasted for 12 h with free access to water, then mice in the experimental group were injected intraperitoneally with fresh streptozotocin (STZ; Sigma, Saint Louis, USA) solution (dissolved in 0.1 mol L⁻¹ citrate buffer, pH 4.5) at a dose of 45 mg kg⁻¹ body weight (bw). Mice in the normal group were injected with citrate buffer. All animals were injected three times every other day. The fasting blood glucose (FBG) levels were detected by OMRON glucose meter (Kyoto, Japan) at 24 h after the last injection. Mice with FBG level over 11.1 mmol L⁻¹ were regarded as type 2 diabetic mice. Type 2 diabetic mice were randomly divided into four groups of ten mice each: model group, low-dose (L-LNE, 75 mg kg⁻¹ bw), medium-dose (M-LNE, 150 mg kg⁻¹ bw), and

high-dose (H-LNE, 300 mg kg⁻¹ bw) LNT treatment group. Mice in the normal and model group were gavage with water daily.

2.4. Blood Sample Collection and Oral Glucose Tolerance Test

FBG and body weight were measured every 2 weeks. After 4 weeks of continuous intragastric administration, all mice were fasted for 12 h with free access to water for oral glucose tolerance test (OGTT). Mice were administrated orally with 2 g kg⁻¹ glucose, then bloods were collected and tested using glucose meter at the times 0, 0.5, and 2 h after glucose administration. Mice were sacrificed by cervical dislocation and the liver, kidney, and cecum were dissected and washed with saline. Part of the liver and kidney were fixed with 10% formaldehyde solution and the rests stored at -80 °C. Ceca were collected directly into autoclaved 1.5-mL germ-free tubes and stored immediately in drikold and later at -80 °C until used. The value of area under curve (AUC) was calculated as follows: $AUC = 0.5 (G_0 h + G_{0.5} h) \times 0.5 + 0.5 (G_2 h + G_{0.5} h) \times 1.5$.

2.5. Histopathological Analysis

The liver and kidney were fixed in 10% formalin. After embedded in paraffin, the organs were cut into 2-mm sections and stained with hematoxylin and eosin. The sections were examined under a light microscope.

2.6. Dynamic Profile of Intestinal Microflora in Response to LNE

The bacterial DNA of intestinal content was extracted using E.Z.N.A. Mag-Bind Stool DNA Kit (Omega, Norcross, USA) following the manufacturer's instructions. The V3-V4 hypervariable domain of 16S rRNA gene were PCR amplified from microbial genome DNA. The primer pairs (Forward: 5'-CCTACGGGNGGCWGCAG-3' and Reverse: 5'-GACTACHVGGGTATCTAATCC-3') were designed. PCR reactions contained 10–20 ng of DNA template, 2 × Taq master Mix (Thermo Scientific, Waltham, MA, USA), 10 μM Bar-PCR primer F, 10 μM Primer R, and H₂O. The following thermal cycling conditions were used: initial denaturation at 94 °C for 3 min; five cycles at 94 °C for 30 s, 45 °C for 20 s, and 60 °C for 30 s; 20 cycles at 94 °C for 30 s, 55 °C for 20 s, and 72 °C for 30 s; and a final extension at 72 °C for 5 min. Amplicons were purified using the Agencourt AMPure XP (Beckman, CA, USA) and quantified using Qubit dsDNA HS Assay Kit (Invitrogen, NY, USA) in accordance with the manufacturers' instructions. Purified libraries were sequenced on the Illumina Miseq platform from Sangon Biotech (Shanghai, China). The bacterial sequence reads were compared to a reference database of known 16S rRNA genes obtained from the Ribosomal Database Project. The bacterial sequences were assigned taxonomically on the basis of the Ribosomal Database Project classifiers. The microbial community structures in different samples were compared using FastUniFrac on the basis of the phylogenetic relationships between representative reads (OTUs) from different samples.

2.7. RNA Extraction and Real-Time PCR

Total RNA from the liver samples of mice was extracted using Trizol reagent (Invitrogen, NY, USA) and reverse transcribed into first-stand cDNA by using cDNA synthesis kit (Takara, Dalian, China). RT-PCR of β-actin, PI3K, and JNK1 was performed using SYBR Green RT-PCR kit (Invitrogen, NY, USA) and the specific primers listed are as follows: β-actin, F: 5'-ACATCCGTAAGACCTCTATGCC-3', R: 5'-TACTCCTGCTTGCTGATCCAC; PI3K, F: 5'-CCAAATGAAAAGAACGGCTA-3', R: 5'-GCGACTTCAGCTTATCATGG-3'; and JNK1 F: 5'-CAGAAGCAAACGTGACAAC-3', R: 5'-AAGAATGGCATCATAAGCTG-3'. Amplifications were performed by the following thermal cycling conditions: 95 °C for 10 min, 95 °C for 15 s, 40 cycles at 60 °C for 50 s. ABI StepOne plus Real-time PCR system (Applied Biosystems, USA) was used to analyze the quantity of the mRNA, which was normalized to that of β-actin.

2.8. Western Blotting Assay

The homogenized hepatic tissues were solubilized by lysis buffer on ice for 30 min. BCA protein assay kit (Beyotime, Shanghai, China) was used to determine the concentrations of lysate protein. The proteins were subjected to SDS-PAGE and were transferred to a polyvinylidene difluoride membrane. The membrane was blocked in blocking buffer (Takara, Dalian, China) at room temperature for 2 h. The membrane was incubated with PI3K, JNK1, or GAPDH (Abcam, Cambridge, UK) rabbit polyclonal antibody and alkaline phosphatase-conjugated goat anti-rabbit IgG (H+L) at 37 °C for 1 h, respectively. The protein blots were visualized using BCIP/NBT Alkaline Phosphatase Color Development Kit (Beyotime, Shanghai, China) and quantified using GeneTools from Syngene software.

2.9. Robust Network from LNE Intake to Antidiabetic Effect

The correlation between LNE, intestinal microflora, physiological indices, and relative genera in pathways were calculated by Spearman's rank correlation coefficient and visualized by network in Cytoscape (Version 3.2.1).

2.10. Statistical Analysis

All values are expressed as mean ± SD. Statistical significance was determined using analysis of variance followed by least significant difference test (LST). A *p*-value less than 0.05 was considered statistically significant.

3. Results

3.1. Characterization of Potent Major Compounds

Phytochemical analysis of LNE led to the isolation of seven major phenolics and flavonoids with background correction

(Supporting Information material 1). Further chromatographic peaks were observed at different retention times from 0.96 to 5.68 min but attempts to unequivocally identify these constituents on the basis of QTOF-MS (Supporting Information material 2). MS analysis confirmed the proposed presence of O-glucuronide derivatives and kaempferol (Supporting Information material 3). The partial fragment ions at m/z are in agreement with previously reported data. Their structures were identified by comparison of their MS spectral data with those reported in the literatures.^[14–16]

3.2. Effect of LNE on Body Weight of Diabetic Mice

On the first day, the body weight of mice in model and LNE treatment group, which was fed with a HSD, were significantly higher than those in normal group ($p < 0.05$) (Supporting Information material 4). When compared with the model control, LNE at medium-dose obviously lowered the body weight after 14 days of administration ($p < 0.05$). Furthermore, the body weight of diabetic mice decreased continually, and on the 28th day, there was no statistically significant difference among all groups ($p > 0.05$). It is noteworthy that a more obvious trend of body weight loss was observed in model group than in LNE treated group.

3.3. Effect of LNE on Fasting Blood Glucose Levels of Diabetic Mice

The effect of LNE on FBG levels in diabetic mice on different days of treatment is shown in Supporting Information material 5. There was no significant difference in FBG level between the diabetic and LNE treatment mice ($p > 0.05$) at the start of the study. However, FBG levels of the diabetic group and LNE groups were significantly higher than those in the normal group ($p < 0.01$). On the 14th day, there was a significant decrease of FBG levels in the three doses of LNE groups compared with diabetic group, without dose-dependent effect ($p < 0.01$). Moreover, the FBG levels in the three LNE groups were similar to those in normal group after 28 days of treatment.

3.4. Effect of LNE on Oral Glucose Tolerance in Diabetic Mice

Glucose tolerance as an indicator plays a crucial role in reflecting the degree of type 2 diabetes. As showed, animal in model group had severely impaired glucose tolerance, and the blood glucose in those animals was obviously higher than in other groups at 0 h (Supporting Information material 6). Lower blood glucose levels were observed both in the medium- and high-dose LNE groups when compared with the model group at 120 min. The AUC of glucose in different groups is shown in Supporting Information material 6. Although, there were significant difference between the normal group and the three LNE ones, LNE treatment significantly decreased the AUC compared with model group ($p < 0.01$). The above results demonstrated that LNE ameliorated the impaired glucose tolerance in diabetic mice.

3.5. Effect of LNE on the Histopathology of Liver and Kidney in Diabetic Mice

Histopathological analyses of the liver and kidney were also conducted (Figure 1). Normal architecture of liver parenchyma was observed in normal group. Local hepatocyte necrosis and moderate portal inflammation were noted in diabetic mice. The hepatocytes morphology of mice treated with LNE at medium and high dose were close to normal level (Figure 1D,E). The results of histopathological examination showed that HSD with STZ damaged the liver of mice. The medium- and high-dose LNE treatment on the liver of mice relieved the hepatocellular damage and inflammation of diabetic mice. The histopathology of kidney showed renal parenchyma with normal tubules and glomeruli in normal mice. However, the cells of kidney tubules showed mild swelling, vacuolar degeneration, and necrosis, and a few inflammatory cells infiltrated in the nephric tubules were observed in diabetic mice. LNE displayed protective effect in high dose treated mice, which were similar to normal architecture of kidney. Furthermore, high-dose of LNE administration relieved the mild inflammation in the kidney of diabetic mice (Figure 1E).

3.6. Effect of LNE on the Structure of Intestinal Microflora in Diabetic Mice

Bacteroidetes, *Firmicutes*, and *Proteobacteria* were the dominant bacteria detected in the intestinal contents of mice at phylum level (Figure 2). Comparing the components of intestinal microflora between diabetic and normal mice, significantly decreased *Bacteroidetes* and *Actinobacteria* populations as well as increased *Firmicutes* were observed in diabetic mice. Medium-dose treatment with LNE significantly increased the abundance of *Bacteroidetes* bacteria and decreased *Firmicutes* populations. *Actinobacteria* populations increased after LNE administration at a low dose. Notably, a higher abundance of *Proteobacteria* was observed in LNE treatment group compared to that without LNE treatment (Figure 2).

The composition of intestinal microflora in type 2 diabetic mice at the genus level was analyzed (Figure 3a). The bacteria in *Barnesiella*, *Clostridium IV*, *Clostridium XIVa*, and *Alistipes* genus changed obviously. Compared with normal group, *Barnesiella* decreased and *Clostridium IV*, *Clostridium XIVa*, and *Alistipes* increased in model group (Figure 3b). Low-dose treatment with LNE significantly increased the population of *Barnesiella*. The abundances of *Clostridium IV*, *Clostridium XIVa*, and *Alistipes* were lower in LNE treatment groups than those in model group (Figure 3b). The structure of intestinal microflora analysis demonstrated that LNE modulated the balance of intestinal microflora in type 2 diabetic mice.

3.7. Effect of LNE on mRNA Expression of PI3K and JNK1 in Liver of Type 2 Diabetic Mice

There was a significant decrease in the mRNA expression level of PI3K gene in diabetic mice when compared with normal mice shown in Figure 4a ($p < 0.01$). LNE treatment could upregulate

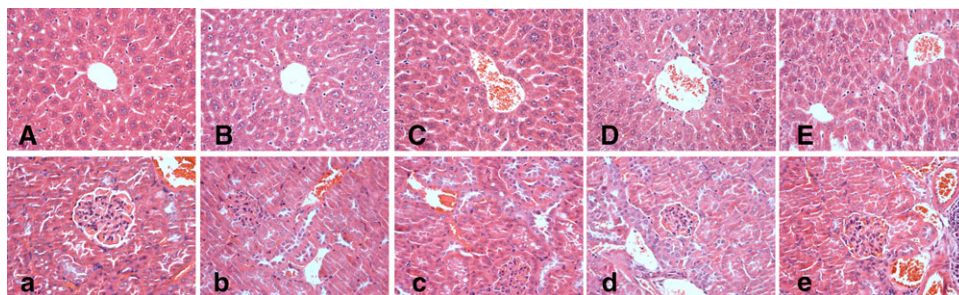


Figure 1. Effect of LNE treatment on the liver A–E) and kidney a–e) of type 2 diabetic mice (Hematoxylin and eosin staining, 400×). A, a) Normal group; B, b) model group; C, c) Low-dose LNE group; D, d) medium-dose LNE group; and E, e) high-dose LNE group.

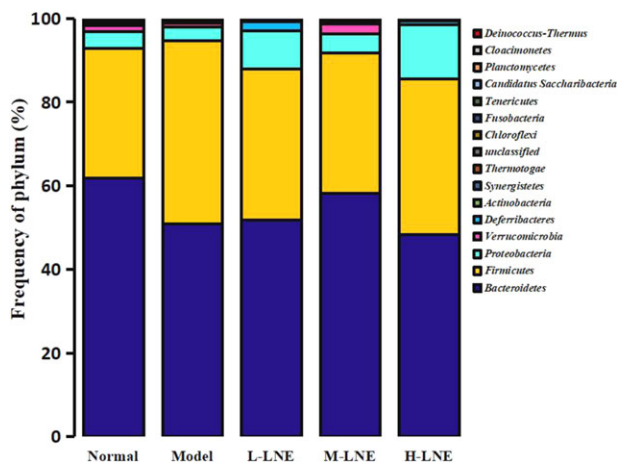


Figure 2. Effects of LNE treatment on the relative abundance of intestinal microflora in type 2 diabetic mice at phylum level.

the expression of PI3K gene ($p < 0.01$). JNK1 gene was significantly upregulated in the liver of diabetic mice compared to normal mice ($p < 0.01$) (Figure 4b). Administration of LNE reduced the gene expression of JNK1 level in a dose-dependent manner ($p < 0.01$). The above results indicate that LNE ameliorated the hepatic insulin resistance in diabetic mice by regulating PI3K and JNK signaling pathway.

3.8. Effect of LNE on Protein Expression of PI3K and JNK1 in Liver of Type 2 Diabetic Mice

To validate the differentially expressed proteins, PI3K and JNK1 were selected for validation by western blotting (Supporting Information material 7). Expression level of PI3K ($p < 0.05$) significantly increased in the LNE group compared with model group mice. In contrast, JNK1 ($p < 0.05$) showed reduced expression after treatment with LNE. These results were consistent with the mRNA expression findings. The mechanism of the hypoglycemic effect of this brown algae might be through modification in the gene and protein expression of hepatic PI3K and JNK1, improving the hepatic insulin resistance, thus promoting the glucose uptake in hepatocyte.

3.9. Robust Network from LNE Intake to Antidiabetic Effect

The LNE intake induced the intestinal microbiome interaction and host antidiabetic effect exhibited the domino effects. A network constructed by LNE, bacterial species, and gene regulatory could better explain their causality (Supporting Information material 8). It could be observed that the intake of LNE promoted the growth of *Barnesiella*, *Helicobacter*, and *Turicibacter*, which were able to stimulate the host's antidiabetic effect, accompanied with the modification in the gene and protein expression of hepatic PI3K and JNK1.

4. Discussion

In this study, *L. nigrescens* was extracted by 55% ethanol for the assessment of antidiabetic activity and intestinal microflora regulation. The present results suggested that LNE treatments marked hypoglycemic activity on STZ-induced diabetic mice fed with HSFD. Also, LNE maintained the normal level of body weight and improved the oral glucose tolerance of type 2 diabetic mice. A wide range of research has provided evidence that intestinal microflora is involved in the onset of insulin resistance and type 2 diabetes by affecting energy balance, glucose metabolism, and low-grade inflammation.^[17] An increase in *Firmicutes* and a decrease in *Bacteroidetes* were found in obese mice,^[18] which was also associated with the pathology of type 2 diabetes and with an increased energy harvest by the host in humans.^[19] Studies revealed that *Firmicutes* promote the caloric absorption from diet and the fat storage in intestinal cells.^[20] The fecal microbiota of mouse was dominated by bacteria, with more than 90% of the species belonging to *Bacteroidetes* and *Firmicutes*, similar to the intestinal microflora in humans.^[21] The abundant changes of the principal bacterial phyla, most notably within the *Firmicutes*, *Bacteroidetes*, and *Actinobacteria* phyla, was observed between normal and diabetic mice in this study. Medium-dose treatment with LNE reversed the alteration of the dominant bacterial composition and would be associated with the antidiabetic effect. *Barnesiella* was one of the most abundant genera detected in mouse intestine.^[22] It was reported that the genus *Barnesiella* is not associated with immune development or inflammatory diseases in the intestine, and that it modulates the composition of the microbiota and optimizes host survival.^[23] The level of *Barnesiella* in the intestine was positively associated with the number of marginal zone B cells and invariant natural killer T cells in the

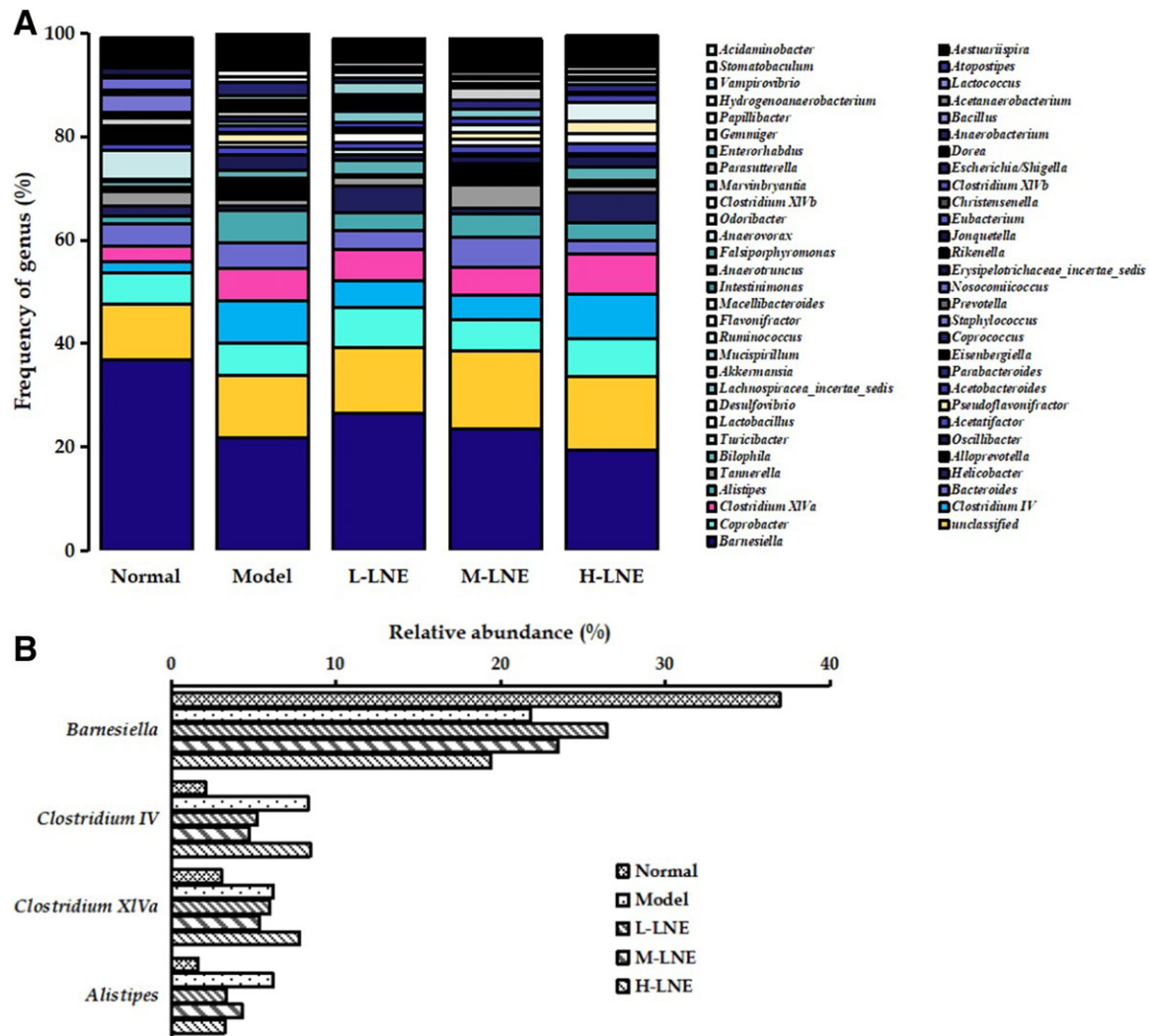


Figure 3. Effects of LNE treatment on the relative abundance of intestinal microflora in type 2 diabetic mice at genus level. a) Distribution barplot of intestinal microflora in genus levels; b) the genus with the largest change in intestinal microflora indifferent groups.

liver.^[24] *Clostridium* species (*Firmicutes* phylum) were negatively correlated to fasting glucose, insulin, and plasma triglycerides.^[25] Remely et al. found that *Clostridium* cluster IV and *Clostridium* cluster XIVa decreased in type 2 diabetic in humans. However, the present study showed an opposite trend in mouse.^[26] *Alistipes*, a bile-tolerant microorganism, is a genus in the phylum *Bacteroidetes*.^[27] *Alistipes* abundance was increased by the animal-based diet.^[28] The present results showed increased population of *Clostridium* cluster IV, *Clostridium* cluster XIVa, and *Alistipes* in diabetic mice, which could be connected to the HSD, while LNE was effective in maintaining the balance of intestinal microflora in mice.

To investigate the mechanisms attributable to the hypoglycemic effect in type 2 diabetic mice, the expressions of the targeted genes and proteins in the insulin signaling pathway were analyzed. Activated JNK inhibits the insulin-stimulated tyrosine phosphorylation of insulin receptor substrate-1, affecting the binding of insulin receptor substrate-1 to downstream molecule, PI3K, thus leading to abnormal insulin transduction. Effective

inhibition of JNK signal transduction represents an important method to improve insulin resistance. The treatment with LNE in diabetic mice showed an increased mRNA expression of PI3K and a decreased JNK1 expression in hepatic cells in comparison with the diabetic mice. The result indicated that the hypoglycemic action of the extract, at least in part, involved the activation of the PI3K signaling pathway and inhibition of JNK signaling pathway to promote the glucose uptake in peripheral tissue.

In conclusion, findings from the present study have verified the antidiabetic effects of LNE in vivo. LNE treatment significantly increased *Bacteroidetes* bacteria and decreased *Firmicutes* populations in intestinal microflora. Specifically, LNE treatment could enrich the amounts of beneficial bacteria, *Barnesiella*, as well as reduce the abundances of *Clostridium* and *Alistipes*. It has been observed that the LNE is also able to mediate through upregulating PI3K and inhibiting JNK1 activity, thereby reducing the concentration of blood glucose. This study provided a new experimental evidence and a new therapeutic window in the prevention and treatment of type 2 diabetes mellitus.

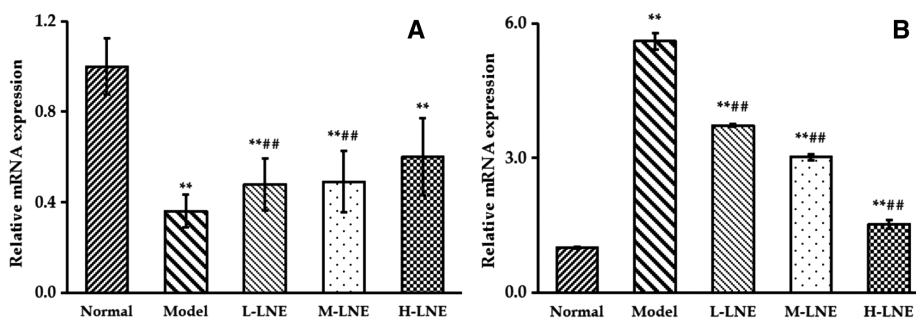


Figure 4. Effects of LNE treatment on the level of phosphatidylinositol 3-hydroxy kinase (PI3K) and Jun N-terminal kinase 1 (JNK1) expression in liver of type 2 diabetic mice. a) Relative expression of PI3K and b) relative expression of JNK1. Values are expressed as mean \pm SD ($n = 10$). Compared with normal group, $**p < 0.01$; compared with model group, $###p < 0.01$.

Abbreviations

AUC, area under curve; FBG, fasting blood glucose; HSFD, high-sucrose/high-fat diet; JNK, c-Jun N-terminal kinase; LNE, *Lessonia nigrescens* ethanolic extract; PI3K, phosphatidylinositol 3-kinase

Supporting Information

Supporting Information is available from the Wiley Online Library or from the author.

Acknowledgments

This work was supported by Natural Science Foundation (2016J06009) and Marine High-tech Industrial Development Project (MIN2014-17) of Fujian Province, China. The project was also supported by Fujian Province Key Laboratory for the Development of Bioactive Material from Marine Algae grant (2017FZSK05), FAFU grants KXb16011A and 612014043.

Conflict of Interest

The authors have declared no conflict of interest.

Keywords

anti-diabetic activity, high-throughput 16S rRNA gene sequencing, intestinal microflora, *Lessonia nigrescens*, signaling pathway

Received: August 24, 2017
Revised: October 29, 2017

- [1] R. Vinayagam, J. B. Xiao, B. J. Xu, *Phytochemistry Rev.* **2017**, *16*, 535.
- [2] J. C. N. Chan, E. Y. K. Chow, A. O. Y. Luk, *Diabetes Mellitus in Developing Countries and Underserved Communities*, (Ed: S. Dagogo-Jack), Springer International Publishing, New York **2017**.
- [3] J. B. Xiao, P. Högger, *Curr. Med. Chem.* **2015**, *22*, 23.
- [4] T. Ozdal, D. Sela, J. B. Xiao, D. Boyacioglu, F. Chen, E. Capanoglu, *Nutrients* **2016**, *8*, 78.
- [5] G. Blandino, R. Inturri, F. Lazzara, D. Rosa, M. Malaguarnera, *Diabetes Metab.* **2016**, *42*, 303.

- [6] F. Navab-Moghadam, M. Sedighi, M. E. Khamseh, F. Alaei-Shahmiri, M. Talebi, S. Razavi, N. Amirrozafari, *Microb Pathogenesis* **2017**, *110*, 630.
- [7] J. C. Clemente, L. K. Ursell, L. W. Parfrey, R. Knight, *Cell* **2012**, *148*, 1258.
- [8] P. M. Vareda, L. L. Saldanha, N. A. Camaforte, N. M. Violato, A. L. Dokkedal, J. R. Bosqueiro, *Evid. Based Complement. Alternat. Med.* **2014**, *2014*, 543.
- [9] J. Hirosumi, G. Tuncman, L. Chang, C. Z. Görgün, K. T. Uysal, K. Maeda, M. Karin, G. S. Hotamisligil, *Nature* **2002**, *420*, 333.
- [10] H. Kaneto, Y. Nakatani, T. Miyatsuka, D. Kawamori, T. A. Matsuoka, M. Matsuhisa, Y. Kajimoto, H. Ichijo, Y. Yamasaki, M. Hori, *Nat. Med.* **2004**, *10*, 1128.
- [11] S. M. Cardoso, O. R. Pereira, A. M. Seca, D. C. Pinto, A. M. Silva, *Mar. Drugs* **2015**, *13*, 6838.
- [12] A. González, J. Beltrán, L. Hiriart-Bertrand, V. Flores, B. de Reviere, J. A. Correa, B. Santelices, *J. Phycol.* **2012**, *48*, 1153.
- [13] I. Gómez, P. Huovinen, *Photochem. Photobiol.* **2010**, *86*, 1056.
- [14] G. Rajauria, B. Foley, N. Abu-Ghannam, *Innov. Food Sci. Emerg.* **2016**, *37*, 261.
- [15] X. Zeng, W. Su, Y. Bai, T. Chen, Z. Yan, J. Wang, M. Su, Y. Zheng, W. Peng, H. Yao, *J. Chromatogr. B Analyt. Technol. Biomed. Life Sci.* **2017**, *1061/1062*, 79.
- [16] B. Amugune, T. K. Milugo, M. Heydenreich, L. K. Omosa, B. Ndunda, A. Yenesew, J. O. Midiwo, *S. Afr. J. Bot.* **2014**, *91*, 58.
- [17] J. Shen, M. S. Obin, L. Zhao, *Mol. Aspects Med.* **2013**, *34*, 39.
- [18] P. J. Turnbaugh, R. E. Ley, M. A. Mahowald, V. Magrini, E. R. Mardis, J. I. Gordon, *Nature* **2006**, *444*, 1027.
- [19] R. Jumpertz, D. S. Le, P. J. Turnbaugh, C. Trinidad, C. Bogardus, J. I. Gordon, J. Krakoff, *Am. J. Clin. Nutr.* **2011**, *94*, 58.
- [20] P. D. Cani, R. Bibiloni, C. Knauf, A. Waget, A. M. Neyrinck, N. M. Delzenne, R. Burcelin, *Diabetes* **2008**, *57*, 1470.
- [21] V. Tremaroli, F. Bäckhed, *Nature* **2012**, *489*, 242.
- [22] G. A. Weiss, C. Chassard, T. Hennen, *Br. J. Nutr.* **2014**, *111*, 1602.
- [23] C. Ubeda, V. Bucci, S. Caballero, A. Djukovic, N. C. Toussaint, M. Equinda, L. Lipuma, L. Ling, A. Gobourne, D. No, Y. Taur, R. R. Jenq, M. R. van den Brink, J. B. Xavier, E. G. Pamer, *Infect. Immun.* **2013**, *81*, 965.
- [24] L. L. Presley, J. Braun, J. Borneman, *Appl. Environ. Microbiol.* **2010**, *76*, 936.
- [25] F. H. Karlsson, V. Tremaroli, I. Nookaew, G. Bergström, C. J. Behre, B. Fagerberg, J. Nielsen, F. Bäckhed, *Nature* **2013**, *498*, 99.
- [26] M. Remely, E. Aumüller, C. Merold, S. Dworzak, B. Hippe, J. Zanner, A. Pointner, H. Brath, A. G. Haslberger, *Gene* **2014**, *537*, 85.
- [27] J. P. Euzéby, *Int. J. Syst. Bacteriol.* **1997**, *47*, 590.
- [28] L. A. David, C. F. Maurice, R. N. Carmody, D. B. Gootenberg, J. E. Button, B. E. Wolfe, A. V. Ling, A. S. Devlin, Y. Varma, M. A. Fischbach, S. B. Biddinger, R. J. Dutton, P. J. Turnbaugh, *Nature* **2014**, *505*, 559.